Defence Science Journal, Vol. 63, No. 4, July 2013, pp. 386-392, DOI : 10.14429/dsj.63.2434

Susceptibility of Electro-explosive Devices to Microwave Interference

John J. Pantoja[*,^], Néstor M. Peña[^], Farhad Rachidi[!], Félix Vega[!,#] and Francisco Roman[#]

[^]*Universidad de los Andes, Cra 1 Nº 18A- 12 Bogotá DC, Colombia*
[!]*Swiss Federal Institute of Technology EPFL, Lausanne, Switzerland*
[#]*Universidad Nacional de Colombia, Bogotá, Colombia*
[*]*E-mail: jj.pantoja28@uniandes.edu.co*

ABSTRACT

In this paper, the electromagnetic susceptibility of electro-explosive devices (EEDs) including their connection wires is assessed statistically. The electromagnetic coupling and the thermal power dissipation are modeled to determine the activation condition due to an excitation with an external electromagnetic field. The reception properties of the connection wires are obtained numerically and validated experimentally; variations in their geometry are considered by means of a Monte Carlo approach. The optimal coupling frequency and the probability of activation of a typical wired EED as function of the magnitude of the excitation are obtained. A detonation probability of 95 per cent is obtained for a wired EED illuminated with a 2447 V/m incident field.

Keywords: Detonator, electro-explosive device, time domain integral equation, electromagnetic interference EMI

1. INTRODUCTION

Electro-explosive devices (EEDs) are commonly used in many industries (e.g. mining, automotive, and military) because of their versatility and simple operation mode. These devices are typically activated by means of a D.C. current applied on their feed wires. However, an unintended activation can be achieved with an external electromagnetic (EM) field coupled to their connection wires. The electromagnetic susceptibility of EEDs has been studied using different strategies in which the feed wires were commonly considered as the element to which the EM field couples, and the EED as its load[1-7]. To determine the characteristics of the electromagnetic field that causes the EED's activation, this problem has been simplified representing the wires as standard antennas with known characteristics (e.g. dipoles and loops)[1-4], applying analyses of worst case based on these canonical structures[1,4-7], and assuming that the system is electrically short[8]. Furthermore, most of the studies have modeled the EED as a pure resistive element with a constant, low resistance. However, EEDs have been shown to be characterized by a frequency-dependent impedance with resonant behavior[9]. Thus, this frequency dependence and, as a consequence, the variable impedance matching between the connection wires and the EED become an important factor to be taken into account in this susceptibility problem[10].

The activation of EEDs due to EM field exposure depends on the intensity and the spectral content of the incident field. Narrow band systems, used to produce Intentional Electromagnetic Interferences (IEMI), can be efficiently used in EED neutralization by taking advantage of the resonant behavior of the EEDs[11]. If the transfer function between the incident field and the dissipated power in the EED is known, optimal coupling frequencies could be derived. Mora[12], *et al.* proposed a methodology to calculate the transfer function including the transient energy conversion into heat inside an EED. It can be applied if the complete system characteristics are known. However, actual circuits with EEDs present connection wires with arbitrary geometries and, as a consequence, arbitrary frequency responses. This randomness in the system calls for a statistical analysis of the problem.

Monte-Carlo approach has been a useful tool to characterize electromagnetic interactions with wires. The response of twisted-wire pairs exited by a plane wave was studied by Armenta[13] *et al.*, where the effect of small random variations of the twisting was analyzed through this method in a wide frequency range. Faster techniques that take advantage of the statistical characteristics of the problem, but with the same principle, have also been proposed. For example, the statistical indicators (i.e. mean, standard deviation and kurtosis) of the induced voltage in an undulating thin-wire over a ground plane have been obtained with a similar method denominated sparse grid[14].

In this paper, the probability of activation of an EED with connection wires with arbitrary geometry and excited by a linearly polarized electromagnetic field is presented. First, the electromagnetic (EM) coupling of a plane wave on an EED with wires is analyzed deterministically. In the third section, a steady state thermal model, based on ANSYS® simulations, to find the activation dissipated power is depicted. In the fourth section, a statistical analysis of the induced power in an EED illuminated with a continuous-wave electric-field and with random configurations of wires is developed with a Monte-Carlo approach. The frequency dependence of the

Received 7 June 2012, revised 7 May 2013, online published 19 July 2013

mean induced power and the survivor function of the samples as a function of the field magnitude are obtained. Finally, a discussion on the obtained results and general conclusions are presented in section five.

2. ELECTROMAGNETIC COUPLING

The coupling between an incident plane wave and the bridge-wire of an EED can be decomposed in two transfer functions[10,12], which correspond to the external interaction and the penetration.

2.1 External Interaction: Plane Wave Excitation

In a differential mode coupling, the connection wires act as receiving antenna and the incident electric field induces currents that feed the EED. Thus, the system (i.e. EED and wires) can be represented by an equivalent circuit, as shown in Fig. 1, in which the EED is represented by a load impedance Z_{EED} and the wires are represented by a Norton equivalent current source I_N with an internal impedance Z_A. Note that the dipole shown in Fig. 1a is only for illustrative purposes.

Although the Norton current source and the source equivalent impedance could be calculated by using analytical expressions for canonical cases (e.g. dipole), the parameters of a wire with arbitrary geometry must be obtained through a full-wave simulation. The time domain integral equation (TDIE) technique with marching on time (MOT) scheme[15] was chosen in this study. The antenna input impedance can be calculated exciting the structure with a voltage source located on the mid-point of the structure, and the induced short circuit current (i.e. Norton current) can be determined by exciting the complete geometry of the wires with an incident plane wave.

The input impedance of the EED was obtained analytically by means of a transmission line model[9], which is based on the EED's diagram presented in Fig. 1a. The EED is modeled by three transmission lines in cascade loaded with the bridge wire. The type of transmission line depends on the structure and materials in each transversal section. The first section at the EED input can be represented by a two-wire line in air, the second, which corresponds to the insulating header, by a twin-axial line in rubber, and the third, the primary explosive section, by another twin-axial line in lead-azide. Knowing the characteristic impedance in each transmission line, the input impedance of each section can be calculated as[17]

$$Z_{in_k} = Z_{o_k} \frac{Z_{L_k} + jZ_{o_k} \tan\theta_k}{Z_{o_k} + jZ_{L_k} \tan\theta_k} \tag{1}$$

where $k = 1, 2, 3$ is the section's number, Z_{o_k} is the section's characteristic impedance, Z_{L_K} is the load impedance, and $\theta_k = (2\pi f / \nu_{p_k})\Delta l_k$ is the section's electrical length. Thus, the load of the last section corresponds to the bridge wire, and the input impedance of the two-wire line section corresponds to the EED's input impedance. The characteristics of the transmission lines used to represent a typical EED[9] are summarized in Table 1.

Figures 2(a) and 2(b) show, as an example, the EED's input impedance as a function of the frequency compared with the simulated input impedance of a 21.3 cm long dipole with a wire diameter of 0.7 mm. The EED presents low impedance at low frequency because, in this range, the impedance value is close to the bridge-wire resistance at DC, which is about 1.3Ω. In contrast, the wires, with impedance Z_A, show high impedance at low frequency due to its open circuit termination. Most connection circuits of EEDs before its activation are open-ended; therefore, the response presented in Figs. 2(a) and

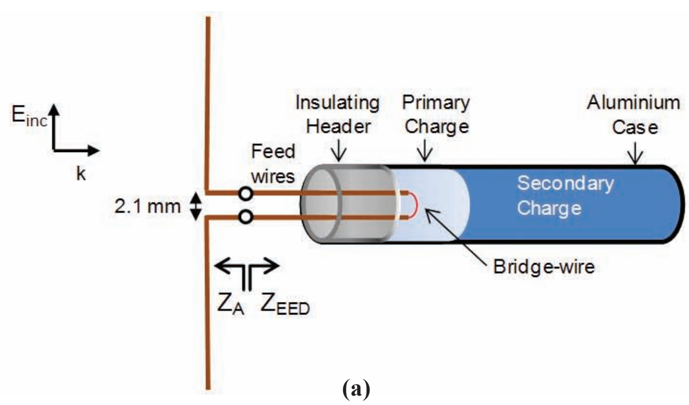

(a)

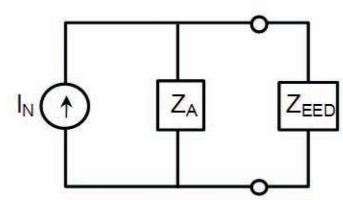

(b)

Figure 1. (a) Diagram and (b) equivalent circuit of an incident plane wave on an EED with connection wires. Typical sections of a hot-wire detonator are depicted.

Table 1. Transmission line parameters of the EED model. Adapted from the work of Lambretch[9], *et al.*

Section	Transmission Line	Δl (mm)	ε_r	Per unit length parameters C (pF/m)	Per unit length parameters L (µH/m)	Z_o (Ω)	υ_p/c
Feed wires	Two-wire	7.9	1	12.13	0.918	275.10	1
Insulating Header	Twin-axial in rubber	37	3	49.90	0.892	133.70	0.50
Primary Charge	Twin-axial in lead-azide	3.3	17	212.07	0.892	64.85	0.24

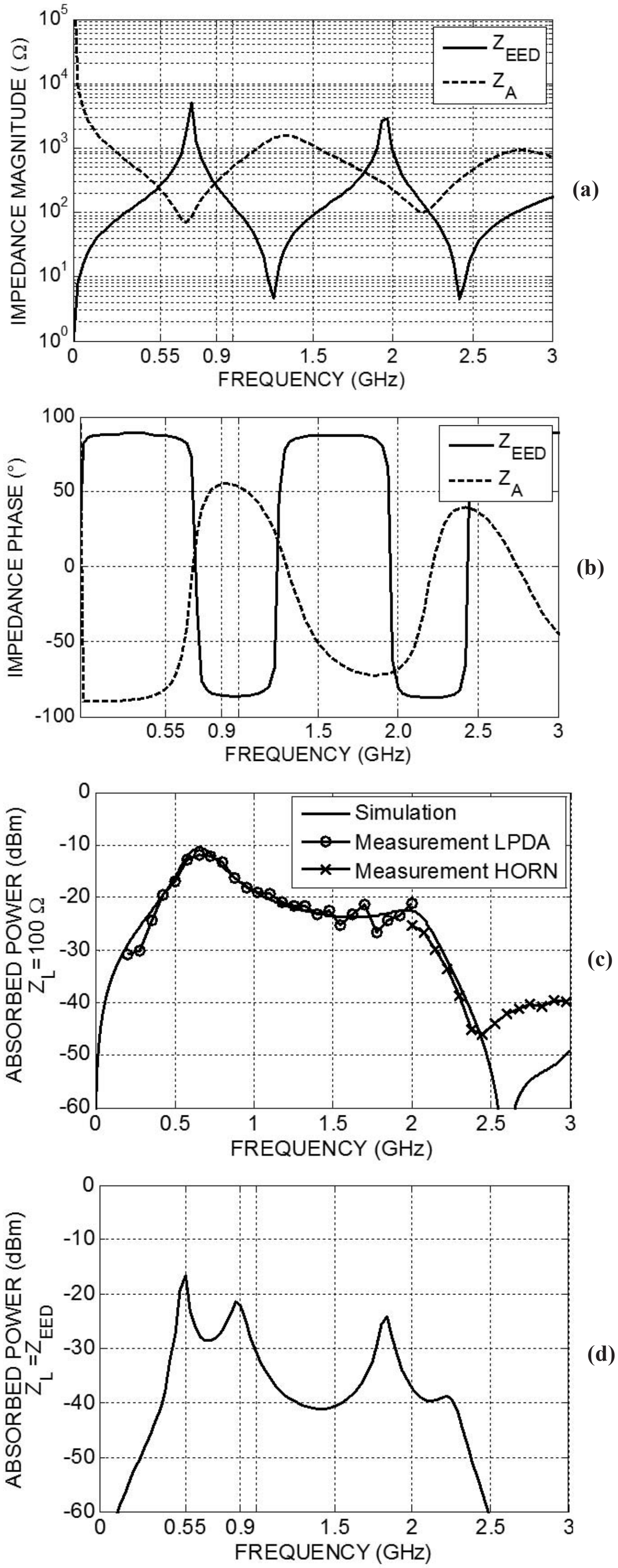

Figure 2. Frequency response of the (a) magnitude and (b) phase of the input impedances of the EED and of the 21.3 cm long wires in dipole configuration. The frequency responses of the power dissipated in a load of (c) 100 Ω and (d) Z_{EED} due to a 1-V/m electric field impinging the wires are also plotted.

2(b) can be considered as typical in most practical cases. The figures also show the resonant behavior of both structures, with alternating phase and magnitude as the frequency increases. As a result, there are multiple frequencies in which the EED's impedance is close to the conjugate complex of the wires' impedance. When this condition is satisfied, the maximum power transfer is obtained in the circuit of Fig. 1(b). The first two frequencies that comply with this condition are 550 MHz and 900 MHz, as depicted in Figs. 2(a) and 2(b).

2.2 Penetration

The actual element in the system that transforms EM energy into heat in the EED is the bridge-wire (see Fig.1(a)). Thus, the activation state depends on the dissipated power on this element. Neglecting the losses in the transmission lines that represent the EED, the power dissipated on the bridge-wire is the same as the one delivered to the input of the EED. Using the Norton equivalent, the power delivered to the EED (P_d) can be obtained using Eqn. (2)[18].

$$P_d = \frac{1}{2}\left|I_N\right|^2 \left|\frac{Z_A}{Z_A + Z_{EED}}\right|^2 \mathrm{Re}\{Z_{EED}\} \tag{2}$$

where I_N is the Norton current, Z_A is the wires' impedance, and Z_{EED} is the EED's input impedance. In addition, considering the wires as an antenna, this power is given by[18]

$$P_d = W_i A_{er} \tag{3}$$

where W_i=$|E_i|^2/(240\pi)$ is the power density of the incident electromagnetic wave, E_i is the incident electric field, and A_{er} is the realized effective area, which only depends on the antenna and load properties. Note that the impedance mismatch and the polarization mismatch losses are included in A_{er}. Thus, the realized effective area corresponds to the transfer function of the electromagnetic coupling between the incident plane wave and the bridge-wire power. A_{er} can be calculated from the power obtained with Eqn. (2) and the known incident electric field.

To verify experimentally the coupling model, the absorbed power in a 100 Ω load connected to the wires of the previous example was measured in an anechoic chamber. The incident plane wave was generated connecting a reference antenna to a port of a vector network analyzer (VNA) with a wideband amplifier. Two reference antennas (Log Periodic Dipole Array LPDA and Double-Ridged Guide Antenna HORN) were used to cover the frequency range between 200MHz and 3GHz. The received power in a balanced port of the VNA was obtained following the procedure presented by Pantoja[16], *et al*. The calculated and measured powers are presented in Fig. 2(c), showing a good agreement.

When the same wires are loaded with the EED, its impedance dependence with the frequency changes the frequency response in the absorbed power. This was calculated with Eqn. (2) and is presented in Fig. 2(d). As expected, the power presents local maxima at the frequencies in which the EED and the wires impedances are matched. In addition, it is possible to see that the global maximum value is obtained in the first matching frequency. That is the effect of the short circuit current frequency response; the power follows the current general tendency of decreasing its magnitude with the frequency.

3. THERMAL DISSIPATION

EEDs, specifically hot-wire detonators, are activated by a deflagration process[19]. When the temperature of the bridge-wire exceeds the autoignition temperature of the primary charge, it detonates and activates the secondary explosive. This critical temperature for the lead azide, a material commonly used as primary charge, is 350 °C[20]. By using a 3D thermal model implemented in ANSYS®, the necessary power dissipated in the bridge-wire to achieve the critical temperature was calculated.

The steady state model includes both natural convective heat transfer with the surrounding air and conductive heat transfer inside the EED. In order to include the natural convection of the air in the simulation, the structure and the surrounding air were implemented in ANSYS® Mechanical APDL application with FLUID142 type elements[21] and the solution was obtained using a FLOTRAN analysis. The dimensions of the simulated EED are given in Table. 1 and the properties of the implemented materials in the thermal model are depicted in Table 2. The model was excited applying a constant power generation condition in the bridge-wire.

Table 2. Thermal Properties of the ANSYS® model

Material	Density (kg/m^{3})	Specific heat (J/kg K)	Conductivity (W/m K)
Air	AIR-SI [a]	AIR-SI [a]	AIR-SI [a]
Aluminum	2702	903	237
Rubber	1000	1800[22]	0.6 [3]
Lead azide	4710	569.02[23]	0.176 [3]
PETN	1770	1138[24]	0.17 [3]

[a] Air material in the ANSYS® FLOTRAN analysis

A power sweep was performed in the simulation to obtain the bridge-wire temperature as a function of the dissipated power. The simulated temperature increment, presented in Fig. 3, shows a linear dependence with the dissipated power with a slope of 973.76 °C/W. Therefore, the temperature increase ΔT can be expressed as

$$\Delta T = R_{th} P_d \tag{4}$$

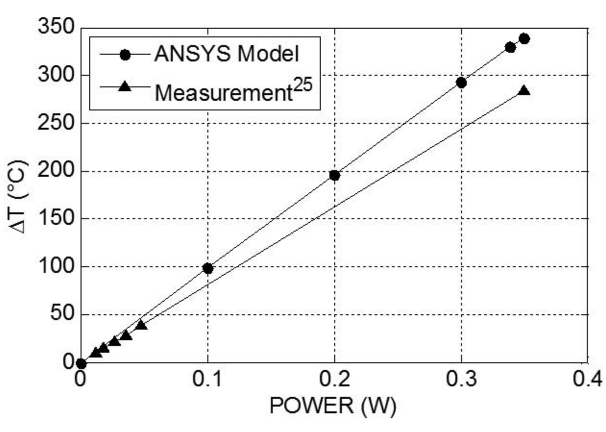

Figure 3. Bridge-wire temperature as function of the dissipated power. The ANSYS® results are compared with the measurements on a 'Type 1' EED[25].

where P_d is the dissipated power and R_{th} is the EED's thermal resistance (i.e. the inverse of the heat loss factor[25]), which corresponds to the slope value of the curve in Fig. 3. With this expression, the temperature due to a given power can be directly calculated and vice-versa. Assuming an ambient temperature of 20 °C and R_{th}= 973.76 °C/W, the critical temperature of the lead azide is obtained with 0.34 W.

For illustrative purposes, the temperature dependence obtained from the experimental data presented by Kankane[25], *et al.* for a 'Type 1' detonator is also plotted in Fig. 3. The detonator 'Type 1' corresponds to a low energy detonator with low no-fire current (<0.3 mA), such as the one simulated in this work. The measurements were made by feeding the detonator with D.C. power values below 0.05 W and by calculating the bridge-wire temperature increase from its resistance change. The curve presented in Fig. 3, with triangular markers, corresponds to the linear extrapolation up to 0.35 W of the measured steady state temperature. Both curves, from ANSYS® simulation and from experimental results, show similar slopes in the linear responses, which was expected since both are low energy devices.

4. STATISTICAL ANALYSIS: WIRES WITH RANDOM GEOMETRIES

4.1 Random Geometries

The variation in the geometries of the connection wires was performed by modifying its length and pattern. Arbitrary patterns were obtained by dividing the wire in sections with equal length but with different inclination angles. Figure 4 shows the six variable angles in the x-y and y-z plane.

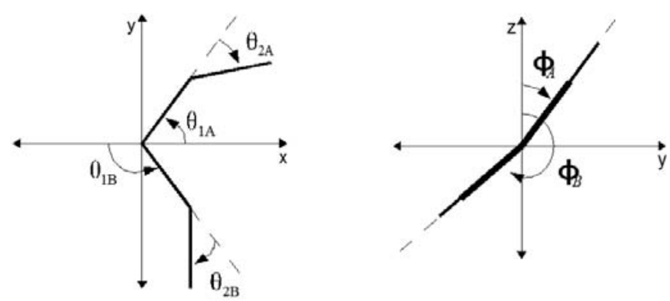

Figure 4. Variable angles for the generation of arbitrary geometries of wires.

A sample of 500 arbitrary wire structures was simulated with TDIE. These configurations aim to represent typical connections of improvised explosive devices (IEDs) and they were obtained by assigning a random uniformly distributed value to the total wire's length and to each inclination angle. The variation range of each variable is presented in Table 3. The electric field was simulated with direction of propagation $\hat{X}$ and polarization $\hat{Y}$. For each case, the short circuit induced current, due to the external incident field, and the wire's input impedance were calculated. With these values and with the EED's input impedance obtained with the transmission line model, the power delivered to the bridge-wire of the EED was calculated by using Eqn. (2).

Table 3. Parameters of the EM Coupling Simulation

Variable	Parameter	Min. value	Max. value
L	Total wire's length	5 cm	25 cm
θ_{1A}, θ_{1B}	Inclination angles θ_{1A} and θ_{1B}	20°	160°
θ_{2A}, θ_{2B}	Inclination angles θ_{2A} and θ_{2B}	-90°	90°
ϕ_A	Inclination angle ϕ_A	20°	160°
ϕ_B	Inclination angle ϕ_B	-20°	-160°
a	Wire's radius	0.7 mm	
$\|E_i\|$	Incident electric field	1 V/m	

4.2 Frequency of Optimal Coupling

An optimal frequency of coupling can be defined when the induced power is the maximum possible for most of the observations. The mean value and the confidence interval of one standard deviation of the induced power in the EED as function of the frequency are presented Fig. 5(a). It clearly shows an optimal frequency range between 500 MHz and 660 MHz in which the mean value of the power increases considerably as compared with the rest of the frequencies.

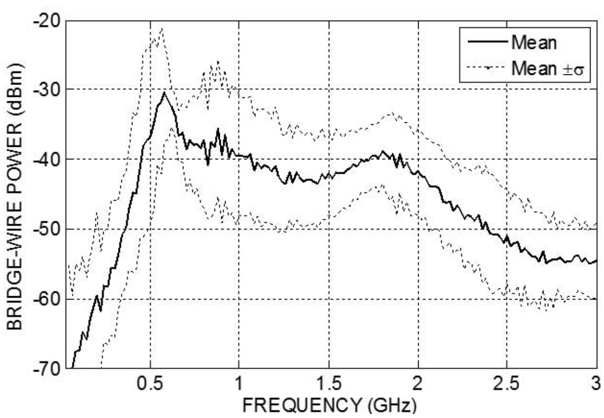

(a)

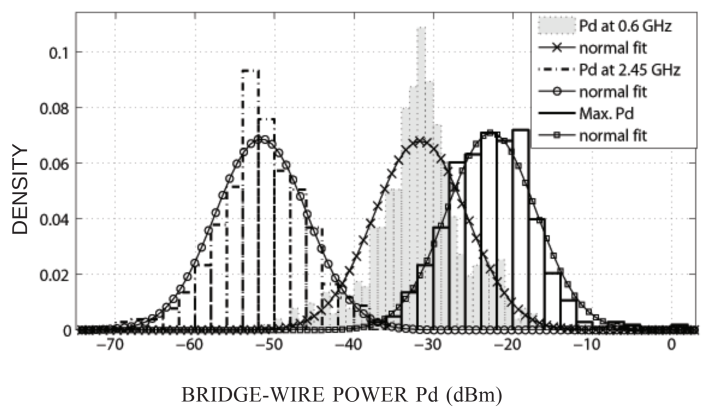

(b)

Figure 5. (a) Mean value and 68.3% confidence interval of the induced power in the bridge-wire of an EED with connection wires with arbitrary geometries as functions of the frequency. (b) Histograms of the induced power for two frequencies: 0.6 GHz and 2.45 GHz. The histogram of the maximum possible induced power is also presented for comparison.

Although the estimated frequency range limits the spectrum in which a good coupling between the incident electric field and the bridge-wire is probable, its bandwidth is wide for a high-power microwave source. For this reason, the best single frequency must be chosen. In Fig. 5(b), the probability density function (PDF) of the induced power in the bridge-wire when the incident electric field has a frequency of 600 MHz is presented. This is compared with the best case, which corresponds to having an electric field able to excite the frequency of maximum coupling of each observation, and with an excitation frequency of 2.45 GHz, which is outside the range of good coupling. The figure shows that a normal distribution can represent each case and that the 600 MHz frequency for the excitation increases considerably the induced power in the bridge-wire compared with an arbitrary frequency outside the found range. The mean value of the 600 MHz distribution is 8.9 dB lower than the mean value of the best case, while the difference between the arbitrary case of 2.45 GHz and the best one is 29.2 dB.

4.3 Magnitude of the Excitation

Now, it is necessary to know the intensity of the field able to induce enough average power to cause a detonation in the observations. To obtain this, the realized effective area of each wire configuration was calculated introducing the simulated power and 1V/m incident field in Eqn. (3). Then, the critical power obtained with ANSYS® (0.34W) was used in the same expression and the magnitude of the electric field necessary to produce the detonation was calculated.

In Fig. 6, the empirical survivor function of the samples when the incident field is tuned at 600 MHz is shown. This figure depicts the probability of a wired EED to bear a specific electric field intensity without detonating. According to these results, the electric field intensity required to detonate 70 per cent of devices is 890 V/m and to detonate the 95 per cent is 2447 V/m.

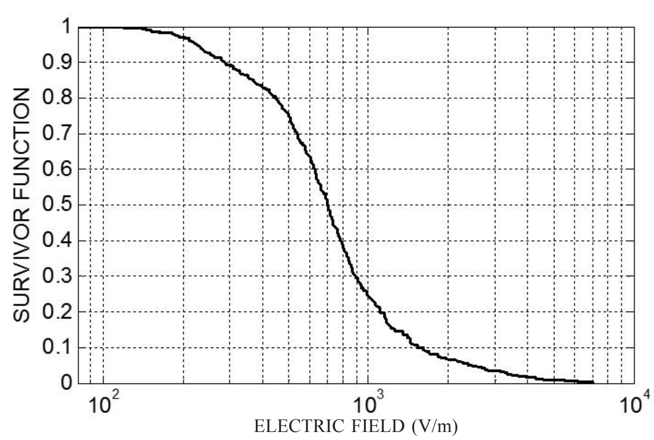

Figure 6. Survivor function of the observations as function of the magnitude of the incident field for a fixed excitation frequency of 0.6 GHz.

5. DISCUSSION AND CONCLUSION

A statistical analysis of the susceptibility of EEDs to microwave radiation was presented. Arbitrary geometries in the connection wires of this device were simulated, creating a set of possible configurations. The frequency dependence of the electromagnetic responses of both the connection wires and the EED was included in a coupling model. Then, the transfer function between an incident electric field with linear polarization and the dissipated power in the EED's bridge-wire was obtained for each sample. Analyzing the probability density of the dissipated power, the optimal coupling frequency of the system for a continuous wave (CW) excitation was calculated. In addition, this power was compared with the critical activation value, which was determined with an ANSYS® steady state thermal model, and the survivor function of a typical EED with connection wires as a function of the magnitude of the incident field was determined.

Here, a CW excitation was considered; therefore, the activation was determined using a comparison between the average power induced due to the CW excitation and the power threshold obtained in ANSYS® with a steady state thermal model. For a transient excitation (e.g. a damped sinusoidal), the EED thermal response could be modeled using a first or second order differential equation[26] and the activation should be determined when the bridge-wire temperature exceeds the critical temperature of the primary charge.

Other factors of the coupling, such as the polarization and the propagation medium, evidently affect the induced power in the EED. The incident wave polarization has a significant effect on the wire's effective area. In this study, the incident wave was assumed to have the same polarization as the average wire's geometry. Although, due to the variability of the geometries, there is always a non-zero probability of inducing antenna currents, a considerable reduction in the mean induced power would be expected if an orthogonal polarization were considered. On the other hand, the simulations were carried out in free space; however, different propagation media can be presented in a real scenario. In the case of a buried device, for example, three main effects should be considered:

(a) a reflection of the incident wave due to change of media
(b) attenuation due to the media losses, and
(c) disturbance of the device's near field due to the properties of the surrounding medium.

As a result, the induced power in the EED would decrease according to the propagation losses. In addition, the frequency dependence of the mean induced power, as shown in Fig. 5 (a), would result modified caused by the effect of the surrounding media on the wire's effective length.

The separation of the problem in the scheme of external interaction and the penetration provides an easier way to bear with devices that have elements with both random and deterministic (typical) responses. This scheme reduces the complexity of the problem since only the variable part of the problem is simulated numerically and the other is calculated analytically. In the implemented model, the connection wires were represented by wire antennas in free space, but in many applications the surrounded material can have different values for the permittivity and losses. For this reason, a future work is to analyze the effect of these parameters in the optimal coupling frequency and in the survivor function.

REFERENCES

1. Heard, N.A.; Strachan, D.C. & Maddocks, A.J. Measurements of the Field strengths on offshore oil platforms for assessing radio-frequency hazards with electro explosive devices. *IEEE Trans. Electromagn. Compat.*, 1985, **27**(3), 162-167.
2. Bishop, A.E. & Knight, P. The safe use of electro-explosive devices in electromagnetic fields. *Radio Electronic Enginee,* 1984, **54**(7.8), 321-335.
3. Parson, J.; Dickens, J.; Walter, J. & Neuber, A. Energy deposition assessment and electromagnetic evaluation of electro-explosive devices in a pulsed power environment. *In* Proceedings of the IEEE Pulsed Power Conference 2009 PPC '09, IEEE, Washington, DC, 2009.
4. Ji-Won Kang; Bierng-Chearl Ahn & Kim, K.J. Evaluation of safety for the 900MHz RFID reader of defense ammunition management system. *In* Proceedings of the International conference on information science and security, ICISS 2008, Seoul, South Korea, 2008.
5. Einstein, H. B. & Warner, H. B. Mathematical evaluation of radio frequency hazards to resistive devices. *IEEE Trans. Electromagn. Compat.*, 1965, **7**(3), 287-296.
6. Baginski, T.A. Hazard of low-frequency electromagnetic coupling of overhead power transmission lines to electro-explosive devices. *IEEE Trans. Electromagn. Compat.,* 1989, **31**(4), 393-395.
7. Thompson, R.H. Safe distances for blasting wiring from commonly encountered underground electromagnetic energy sources. Franklin Research Center, Technical Report C5490, Philadelphia, PA. September 1983.
8. Li, G.L.; Li, G.X.; Wang, P.L. & Lao, Y.L. Study on absorption power of electrical small EED in RF hazard. *In* Proceedings of the International Symposium on Safety and Technology, Progress in Safety Science and Technology, Beijing, China, 2008.
9. Lambrecht, M.R.; Cartwright, K.L.; Baum, C.E. & Schamiloglu, E. Electromagnetic modeling of hot-wire detonators. *IEEE Trans. Micro. Theory Tech.*, 2009, **57**(7), 1707-1713.
10. Pantoja, J.; Peña, N.; Román, F.; Vega, F. & Rachidi, F. A study on the electromagnetic susceptibility of improvised explosive devices**.** *In* the Abstracts of the European Electromagnetics International Symposium EUROEM 2012, SUMMA Foundation, Toulouse, France, 2012.
11. Devarapalli, N.R.; Baum, C.E.; Christodoulou, C.G. & Schamiloglu, E. A fan-beam radiator using waveguide's narrow wall for horizontal polarization and high power. . *IEEE Trans. Electromagn. Compat.*, 2011, **53(**2), 380-389.
12. Mora, N.; Rachidi, F.; Peña, N. & Roman, F. Modeling of the electromagnetic coupling to electro-explosive devices**.** *In* Proceedings of the URSI General Assembly and Scientific Symposium 2011, XXXth, URSI, Istanbul, Turkey, 2011.
13. Armenta, R.B. & Sarris, C.D. Modeling the terminal response of a bundle of twisted-wire pairs excited by a plane wave. *IEEE Trans. Electromagn. Compat.*, 2007, **49**(4), 901-913.

14. Sy O.O.; Van Beurden M.C.; Michielsen B.L.; Vaessen J.A. & Tijhuis A.G. A statistical characterization of resonant electromagnetic interactions with thin wires: Variance and kurtosis analysis. *In* Scientific Computing in Electrical Engineering SCEE 2008, Mathematics in Industry, *edited by* J. Roos & L.R.J. Costa. Springer, Berlin, Germany, 2010, **14**, pp. 117-124.
15. Rao, S.; Sarkar, T. & Dianat, S. A novel technique to the solution of transient electromagnetic scattering from thin wires. *IEEE Trans. Antennas Propag.,* 1986, **34**(5), 630- 634.
16. Pantoja, J.; Peña, N.; Román, F.; Vega, F.; & Rachidi, F. Wideband experimental characterization of differential antennas. *In* Proceedings of the sixth European conference on Antennas and Propagation (EuCAP 2012), IEEE, Prague, Czech Republic, 2012.
17. Pozar, D.M. Transmission line theory. *In* Microwave Engineering, Third edition. John Wiley & Sons, New York, 2004. pp. 82-83.
18. Best, S.R. & Kaanta, B.C. A tutorial on the receiving and scattering properties of antennas. *IEEE Antennas Propag. Mag.,* 2009, **51**(5), 26-37.
19. Varesh, Ron. Electric Detonators: EBW and EFI. *Propellants, Explosives, Pyrotechnics*, 1996, **21**(3), 150–154.
20. Eggert, J. The ignition of explosives by radiation. *J. Phys. Chem.*, 1959, **63**(1), 11–15.
21. Garman, R.W. A CFD assessment of heat transfer through a ship's Hull. *In* Proceedings of the 2002 Int. ANSYS Conf., ANSYS, Pittsburgh, PA, 2002.
22. Richardson, M.J. tables of physical & chemical constants. Kaye & Laby, National Physical Laboratory. http://www.kayelaby.npl.co.uk/general_physics/2_3/2_3_6.html [Accessed on 6 June 2011]
23. Stolovy, A.; Kidd, J. Thermal initiation of confined primary explosives with a proton beam. Naval Research Laboratory, United States Navy, NRL Memorandum Report No. 6558. September 1989.
24. Jones, D.A. & Parker, R.P. Simulation of Cookoff results in a small scale test. Explosives Ordnance Division, Aeronautical and Maritime Research Laboratory, Technical Report No. AR-008-959. October 1994.
25. Kankane, D. K.; Ranade, S. N.; Sohoni R. B. & Deshpande G. S. instrumentation system for thermal analysis of electro-explosive devices. *Def. Sci. J.*, 1999, **49**(1), 31-39.
26 Pantoja, J.J.; Pena, N.; Mora, N.; Rachidi, F.; Vega, F. & Roman, F. On the electromagnetic susceptibility of hot wire-based electroexplosive devices to RF sources. *IEEE Trans. Electromagn. Compat.*, 2012, **PP**(99), 1-10.

Contributors

Mr John J. Pantoja received his BS (Electronics Engineering) from the National University of Colombia, Colombia in 2008. Currently he is pursuing his PhD (Electrical Engineering) at the Universidad de los Andes, Bogotá, Colombia. His research areas include : Electromagnetic compatibility, intentional electromagnetic interference, and computational electromagnetics.

Dr Nestor Peña received his MSc (Electrical Engineering) from Universidad de los Andes, Bogotá, Colombia and PhD (Signal Processing and Telecommunications) from Université de Rennes I, Rennes, France. He is the head of the Group of Electronic and Telecommunication Systems and Associate Professor at Department of Electrical and Electronics Engineering, Universidad de los Andes. His interest areas include : Numerical modeling, high-frequency and microwave electronics, and communication networks.

Dr Farhad Rachidi received MS (Electrical Engineering) and PhD from the Swiss Federal Institute of Technology, Lausanne, in 1986 and 1991 respectively. He is currently head of the EMC Laboratory at the Swiss Federal Institute of Technology, Lausanne, Switzerland. He is the author or coauthor of over 300 scientific papers published in reviewed journals and presented at international conferences. In 2005, he was the recipient of the IEEE Technical Achievement Award and the CIGRE Technical Committee Award. He was awarded the 2006 Blondel Medal from the French Association of Electrical Engineering, Electronics, Information Technology and Communication (SEE).

Dr Felix Vega received his PhD (Electrical engineering) (with honors) from the National University of Colombia, Colombia, in 2011. He has also received PhD (Electrical Engineering) at the Swiss Federal Institute of Technology of Lausanne, Switzerland in 2013. He is currently an Assistant Professor in the National University of Colombia. His research areas include : Generation and radiation of fast rise-time high power electromagnetic signals, intentional electromagnetic interference, and pulsed power.

Dr Francisco Román received his PhD (Electricity) from the University of Uppsala, Sweden, in 1997. He received the Phil. Lic. from Uppsala University. He has three patents in the U.S. and one in Colombia. He invented the Roman Generator. He is currently a full Professor and the main researcher of the EMC research group at the National University of Colombia. He is a member of the CIGRE WG C4.04.01 on Lightning Protection (SIPDA). He received in 2005 the Colombian prize 'Alejandro Ángel Escobar'.